

# COLLAPSE OF HOLLOW PYRAMIDAL LATTICE MATERIAL UNDER QUASI-STATIC LOADING

Shivnandan M. Pingle<sup>1</sup>, Norman A. Fleck<sup>1</sup>, Haydn N.G. Wadley<sup>2</sup>

<sup>1</sup> Department of Engineering, University of Cambridge, Trumpington Street, Cambridge, CB2 1PZ, UK

<sup>2</sup> Department of Materials Science and Engineering, University of Virginia, 116 Engineers Way, Charlottesville, VI 22904, USA  
Email address: smp56@cam.ac.uk

## ABSTRACT

The quasi-static response of hollow pyramidal lattice material under compression and shear is predicted by finite element analysis. The dependence of the collapse mode upon the geometry of the inclined pyramidal struts is explored. A set of collapse modes are identified for compressive and shear loadings. The numerical predictions give additional insight into the measured quasi-static responses.

## 1. Introduction

Lattice materials are periodic micro-architected cellular solids in which the individual elements deform by stretching rather than by bending. Consequently, the stiffness and strength of lattice materials scale linearly with their relative density ( $\bar{\rho}$ ) and so they compete favourably with metal foams as the cores of sandwich panels [1]. Lattice truss topologies (kagome, tetragonal and pyramidal) are generally composed of solid struts made from ductile alloys. Recently, it has been demonstrated experimentally that hollow truss cores (in diamond and square orientations) offer structural advantage over their solid truss counterparts [2,3]. The increase in compressive strength is associated with their enhanced buckling resistance [3,4]. However truss-based lattice materials suffer from two major drawbacks:

(i) The bonded area between the core and the face sheets may not be sufficient to enable the transfer of forces from core to face sheet and to prevent debonding failure [5,6].

(ii) The conventional manufacturing method of node row folding fails to utilize initial sheet material efficiently, especially at lower relative densities.

Wadley has developed an alternative manufacturing method (tube insertion method) which tackled both shortcomings [7]. The assembly process during tube insertion method and a brazed sandwich panel are sketched in Fig. 1(a)-(b). This method ensures efficient material usage and allows for a robust node design. Sandwich structures with hollow pyramidal core made from ( $\bar{\rho}=0.9 - 5.8\%$ ) annealed AISI type 304 stainless steel have been fabricated in this manner, and their through thickness compressive and transverse shear strengths were measured [6]. Various plastic buckling modes were observed as a function of tube geometry.

In this paper, we first identify the dominant non-dimensional groups for defining the geometry of hollow pyramidal lattice material. Then, we use the finite element (FE) method to predict the elasto-plastic collapse response of hollow pyramidal lattice material under compressive and shear loadings. The competing collapse modes are identified for compression and shear loading as a function of geometric variables.

The numerical results are compared with experimental data of Queheillalt and Wadley [6]: excellent agreement is noted.

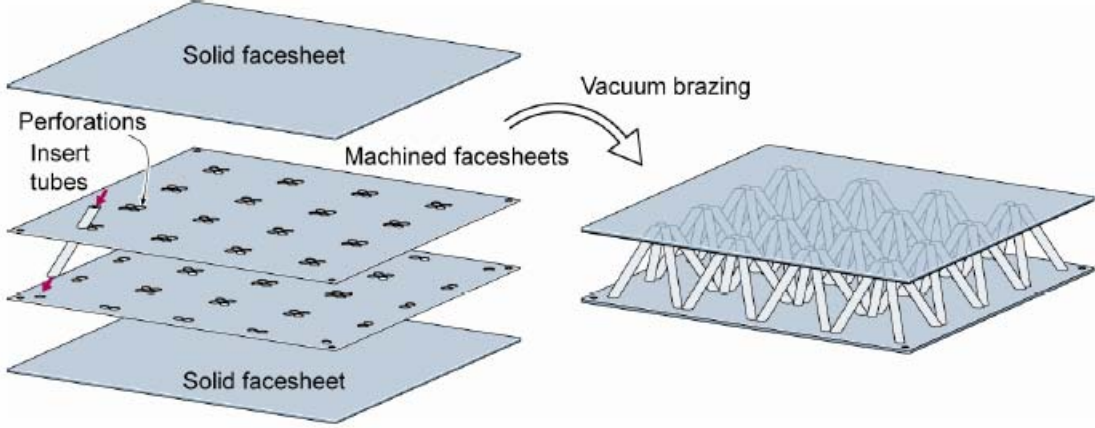


Fig. 1: The tube insertion method. Tubes were inserted in the face sheets and the sandwich panel was assembled.

## 2. Geometry of pyramidal lattice made from tubes

A unit cell of the hollow pyramidal lattice material, consisting of four inclined circular tubes, is shown in Fig. 2. The geometry is defined in terms of the wall thickness  $t$ , outer diameter of tube  $d_o$  and height  $h$  of the core. The axis of neighbouring tubes is spaced a distance  $S=2d_o$  at the faces, as shown in Fig. 3a. The relative density  $\bar{\rho}$  of the lattice core is a function of  $t/d_o, h/d_o$  and the inclination  $\omega$  of each tube. Write the yield strength of the fully dense solid as  $\sigma_y$  and the compressive collapse strength of the sandwich as  $\sigma_{pk}$ . The non-dimensional compressive strength of the sandwich is defined as  $\bar{\sigma} = \sigma_{pk}/(\bar{\rho}\sigma_y)$  and also depends upon  $t/d_o, h/d_o$  and  $\omega$ . In the experimental study of Queheillalt and Wadley [6],  $\omega$  and  $d_o$  are held constant and  $t$  and  $d_i$  are varied for a selected number of tubes. The relative density depends upon the geometry according to

$$\bar{\rho} = \frac{\pi(4d_o t - 4t^2)}{(\sqrt{2} h \cot \omega + 4d_o)^2 \sin \omega} \quad (1)$$

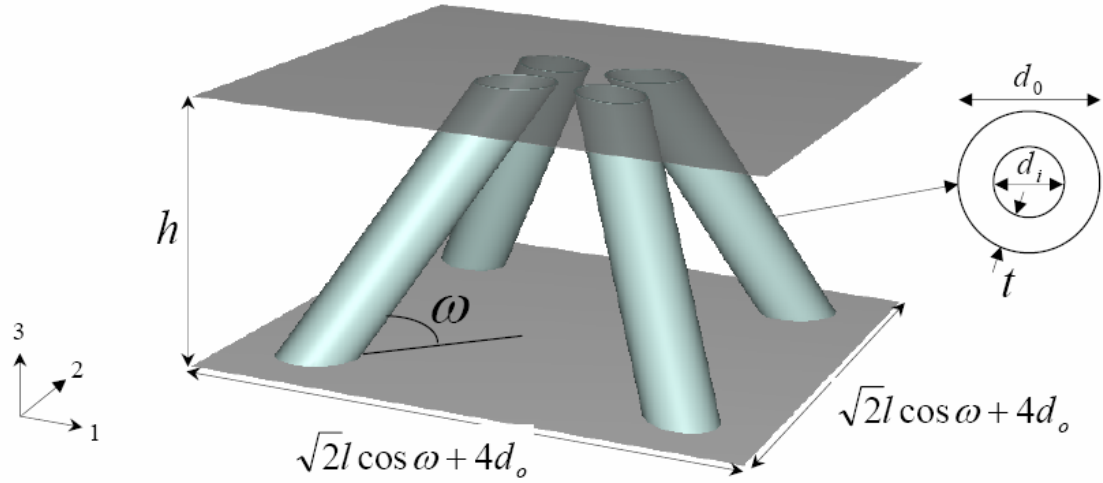


Fig. 2: Unit cell of pyramidal core,  $\omega = 55^\circ$ .

Compression tests and shear tests were performed, as sketched in Fig. 3.

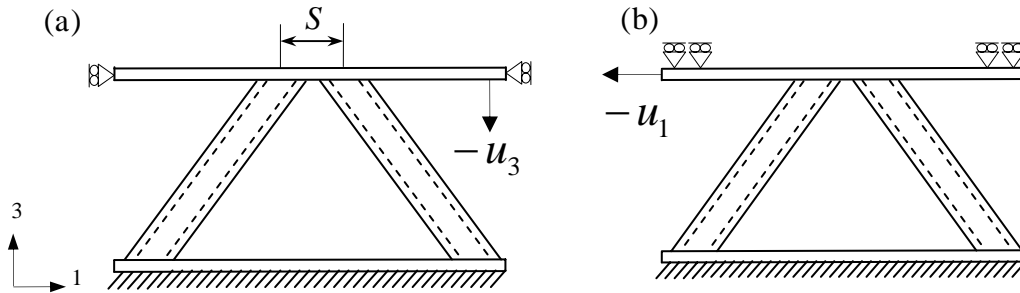


Fig. 3: Boundary conditions for the hollow pyramidal unit cell in 2D, in (a) compression and (b) shear.

### 3. Finite element modelling of hollow pyramidal core

Nonlinear finite element simulations were performed using of implicit version of commercial finite element software, ABAQUS/Standard. The tubes were meshed with 8-noded hexahedral linear element (C3D8R in ABAQUS notation) employing reduced integration. Five elements were required in the thickness direction in order to capture the buckling modes. A mesh convergence study showed that 40,000-50,000 elements were required per tube. The self contact option of ABAQUS was used to prevent self penetration. The two face sheets were represented by rigid surfaces. For compressive loading, only one inclined tube was modeled while in the case of shear loading, two adjacent inclined tubes were modeled. The bottom face sheet remained clamped for both types of loading. The symmetry of the pyramidal core implies that the longitudinal and transverse shear responses are identical.

A measured material response of the annealed AISI type 304 stainless steel was used in the ABAQUS simulations. The tensile tests were performed on sheet material that

had been subjected to the same thermal cycle as that employed during fabrication of the brazed sandwich structures [6]. The annealed stainless steel samples exhibited significant strain hardening as shown in Fig. 4, and  $J_2$  flow theory was employed. The simulations were performed subject to displacement-control loading, using large deformation capability (NLGEOM) to capture post-buckling response [8]. No imperfections were introduced in the finite element model.

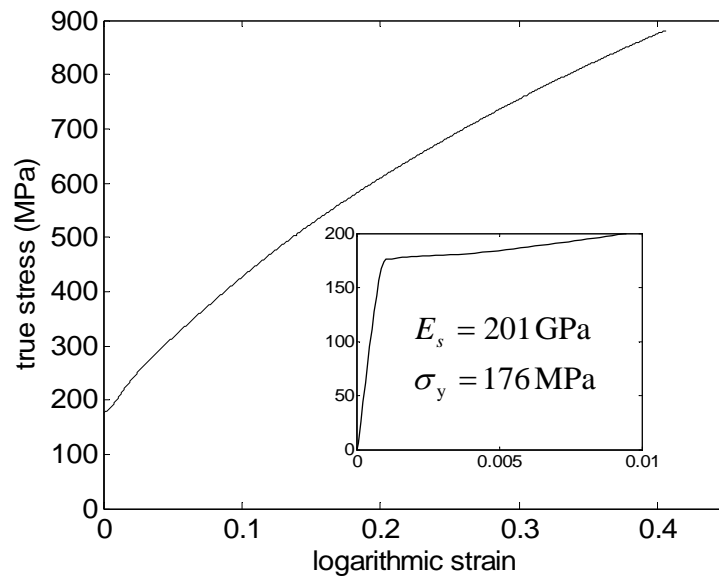


Fig. 4: Measured tensile stress versus strain curve of the annealed AISI type 304 stainless steel.

#### 4. Collapse modes

A set of collapse mechanisms was observed when the hollow pyramidal core was subjected to compressive and shear loadings. The experimentally observed buckling modes [6] are shown in Tables 1 and 2, and the corresponding nominal stress-strain responses of the core are shown in Fig. 5 (dashed line).

##### 4.1 Deformed shapes under compression

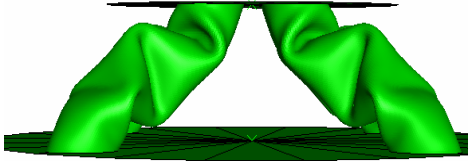



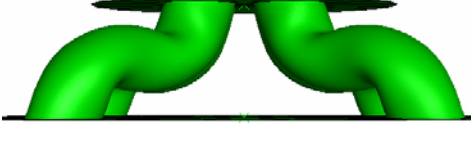
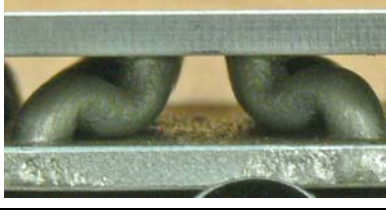

Table 1 includes images of the predicted and observed collapse modes for compression.

Mode 1. This collapse mode is observed in thin, slender inclined tubes, associated with low  $\bar{\rho}$ . A series of creases form in each tube, with neighbouring creases perpendicular to each other.

Mode 2. This collapse mode is observed at intermediate values of  $t/d_o$  and  $h/d_o$  ratios. Neighbouring creases are parallel to each other.

Mode 3. This plastic buckling mode occurs in solid inclined struts.

Mode 4. Short tubes buckle in this manner.

Collapse mode details	FE prediction	Experimental result
Mode 1 $\bar{\rho} = 0.93\%$ $\left(\frac{t}{d_o} = 0.04, \frac{h}{d_o} = 4\right)$		
Mode 2 $\bar{\rho} = 1.78\%$ $\left(\frac{t}{d_o} = 0.08, \frac{h}{d_o} = 4\right)$		
Mode 3 $\bar{\rho} = 3.25\%$ $\left(\frac{t}{d_o} = 0.16, \frac{h}{d_o} = 4\right)$		
Mode 4 $\bar{\rho} = 3.25\%$ $\left(\frac{t}{d_o} = 0.16, \frac{h}{d_o} = 4\right)$		<p style="text-align: center;"><b>Experimental result not available</b></p>
<p>Table 1: Comparison between predicted and experimentally observed deformed shapes of hollow pyramidal lattice core under compression.</p>		

## 4.2 Deformed shapes under shear

Now collapse of hollow pyramidal lattice material under shear loading is considered. Depending on the geometry, the compressed member shows distinct deformation modes. Table 2 includes images of the predicted and observed collapse modes for shear.

Mode 1. A thin inclined tube buckles under combination of torque and compression and exhibit chessboard deformation pattern.

Mode 2. This collapse mechanism is observed in long inclined tubes. An inclined tube gets folded under torsion and compression and the axes of creases are at an angle to each other.

Mode 3. This plastic buckling mode occurs in solid inclined struts.

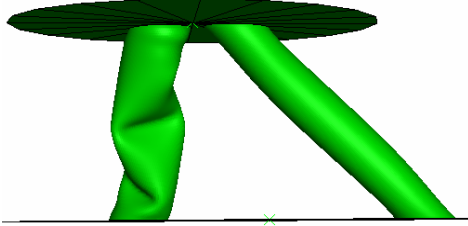

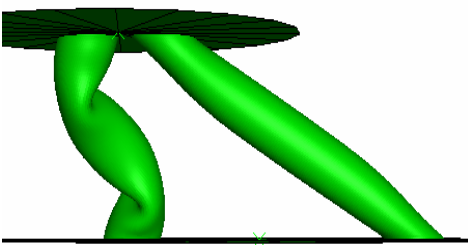

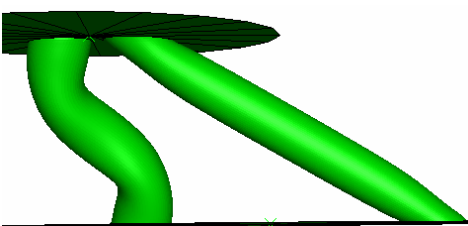

Collapse mode details	FE prediction	Experimental result
Mode 1 $\bar{\rho} = 0.93\%$ $\left(\frac{t}{d_o} = 0.04, \frac{h}{d_o} = 4\right)$		
Mode 2 $\bar{\rho} = 1.78\%$ $\left(\frac{t}{d_o} = 0.08, \frac{h}{d_o} = 4\right)$		
Mode 3 $\bar{\rho} = 3.25\%$ $\left(\frac{t}{d_o} = 0.16, \frac{h}{d_o} = 4\right)$		

Table 2: Comparison between predicted and experimentally observed deformed shapes of hollow pyramidal lattice core under shear.

## 5. Predicted response of core

### 5.1 Compressive response

The predicted nominal compressive stress-strain responses of cores with these configurations are shown in Fig. 5a. As expected the strength increases with  $\bar{\rho}$ . The peak stress is attained at an increasing value of imposed strain with increasing  $\bar{\rho}$ .

The predicted response comprises an initial elastic behaviour, followed by homogeneous plastic deformation and then plastic buckling. This is followed by a decrease in the load carrying capacity.

## 5.1 Shear response

The nominal shear stress-strain responses of these configurations are shown in Fig. 5b. During shear, the elastic behaviour during initial loading is observed followed by yielding of the core and hardening of the core until peak shear stress is reached. The peak stress is attained at an increasing value of imposed strain with increasing  $\bar{\rho}$ .

Under both forms of loading, numerical predictions of the deformed shapes and nominal stress-strain responses agree well with measurements, see Tables 1 and 2, and Fig. 5.

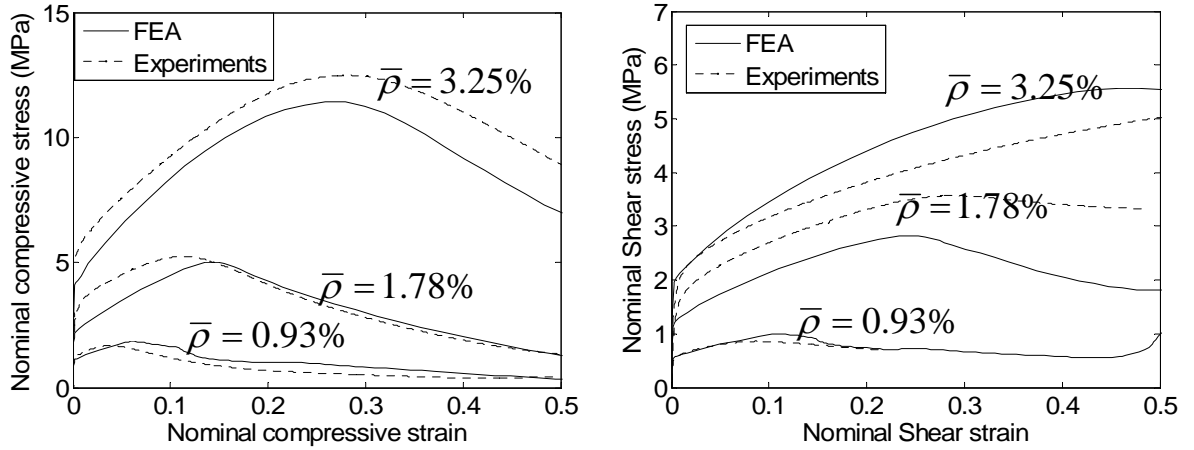


Fig. 5: (a) Nominal compressive stress-strain response and (b) Nominal shear stress-strain response (Refer Table 1 and 2 for collapse mode details).

## 6. Concluding remarks

Numerical simulations have been performed to predict the mechanical response of hollow pyramidal lattice material (made of annealed stainless steel 304) under compression and shear. Distinct collapse mechanisms are identified by varying thickness and height of the hollow pyramidal core. The observed deformation mechanisms and nominal stress-strain responses agree with the finite element predictions.

## Acknowledgements

The authors are grateful for financial support from the EPSRC contract EP/D055806/1 and the ONR contract N00014-07-10114.

## References

- [1] Deshpande, V.S., Fleck, N.A. (2003). Energy absorption of an egg-box material. *Journal of Mechanics and Physics of Solids*, 51, 187-208.
- [2] Queheillalt, D.T., Wadley H.N.G. (2005). Cellular metal lattices with hollow trusses, *Acta Materialia*, 53, 303-313.

- [3] Queheillalt, D.T., Wadley, H.N.G. (2005). Pyramidal lattice truss structures with hollow trusses, *Material Science and Engineering A*, 397, 132-137.
- [4] Timoshenko, S.P., Gere J. M., (1961). *Theory of elastic stability*. McGraw-Hill.
- [5] Kooistra, G. W., Wadley H. N. G. (2007). Lattice truss structures form expanded metal sheet, *Materials and Design*, 28, 507, 514.
- [6] Queheillalt, D.T., Wadley, H.N.G. (2007). Experimental investigation of quasi-static response of hollow pyramidal lattice truss structures, Internal Report, IPM, University of Virginia. To be published.
- [7] Wadley, H.N.G. (2006). Multifunctional periodic cellular metals, *Philosophical Transactions of Royal Society A*, 364, 31-68.
- [8] Abaqus (2006), *Abaqus Version 6.6 Reference Manuals*, Abaqus Inc., Providence, R.I.